doi:10.1016/j.jmb.2009.02.029 J. Mol. Biol. (2009) 388, 30–47

JMB

Available online at www.sciencedirect.com

ScienceDirect

ELSEVIER

Mechanism Analysis Indicates that Recombination Events in HIV-1 Initiate and Complete Over Short Distances, Explaining Why Recombination Frequencies Are Similar in Different Sections of the Genome

Sean T. Rigby[1], April E. Rose[1], Mark N. Hanson[1] and Robert A. Bambara[1,2]*

[1]*Department of Biochemistry and Biophysics, University of Rochester School of Medicine and Dentistry, Rochester, NY 14642, USA*

[2]*Wilmot Cancer Center, University of Rochester Medical Center, Rochester, NY 14642, USA*

Received 15 December 2008; received in revised form 9 February 2009; accepted 12 February 2009
Available online 20 February 2009

Strand transfer drives recombination between the co-packaged genomes of HIV-1, a process that allows rapid viral evolution. The proposed invasion-mediated mechanism of strand transfer during HIV-1 reverse transcription has three steps: (1) invasion of the initial or donor primer template by the second or acceptor template; (2) propagation of the primer–acceptor hybrid; and (3) primer terminus transfer. Invasion occurs at a site at which the reverse transcriptase ribonuclease H (RNase H) has created a nick or short gap in the donor template. We used biochemical reconstitution to determine the distance over which a single invasion site can promote transfer. The DNA-primed RNA donor template used had a single-stranded pre-created invasion site (PCIS). Results showed that the PCIS could influence transfer by 20 or more nucleotides in the direction of synthesis. This influence was augmented by viral nucleocapsid protein and additional reverse transcriptase-RNase H cleavage. Strand-exchange assays were performed specifically to assess the distance over which a hybrid interaction initiated at the PCIS could propagate to achieve transfer. Propagation by simple branch migration of strands was limited to 24–32 nt. Additional RNase H cuts in the donor RNA allowed propagation to a maximum distance of 32–64 nt. Overall, results indicate that a specific invasion site has a limited range of influence on strand transfer. Evidently, a series of invasion sites cannot collaborate over a long distance to promote transfer. This result explains why the frequency of recombination events does not increase with increasing distance from the start of synthesis, a characteristic that supports effective mixing of viral mutations.

Keywords: HIV-1; reverse transcriptase; strand transfer; recombination; hybrid propagation

Edited by J. Karn

Introduction

Recombination during reverse transcription is a source of genetic diversity in HIV-1. During reverse transcription, mutations are frequently generated.[1–8] Differing co-packaged RNA genomes can recombine an advantageous genetic code, resulting in improved viral fitness.[9–15] Reverse transcriptase (RT) is the enzymatic protagonist of reverse transcription. The two catalytic activities of RT are polymerization and ribonuclease (RNase) H (i.e., cleavage of RNA strands that are annealed to DNA).[16–19] Through these two activities, RT reverse transcribes double-stranded DNA from the genomic single-stranded RNA templates. Successful completion of reverse transcription requires strand transfer, a process by which the nascent DNA switches between RNA templates.[20] Through strand transfer, sequence variations between co-

**Corresponding author.* Department of Biochemistry and Biophysics, University of Rochester School of Medicine and Dentistry, Rochester, NY 14642, USA. E-mail address: robert_bambara@urmc.rochester.edu.

Abbreviations used: RNase, ribonuclease; PCIS, pre-created invasion site; RT, reverse transcriptase; NC, nucleocapsid protein; ssDNA, single-stranded DNA; PBS, primer binding site; D_{RNA}, donor RNA; WT, wild type; D_{DNA}, donor DNA.

packaged RNA genomes can be combined in the double-stranded DNA product.

Strand-transfer recombination can occur at any time during minus-strand synthesis, as described by the "dynamic copy choice" model, and recombination is dependent on the ratio between rates of RNA cleavage and DNA synthesis.[21–23] A ratio in favor of RNA cleavage produces higher efficiency of strand transfer, while less cleavage and an increased rate of polymerization favor a lower transfer efficiency. Results of many experiments performed both *in vivo* and *in vitro* indicate that cleavage of the RNA leads to an "invasion-mediated" mechanism of strand transfer—a process in which a second RNA invades gaps in the initial RNA template to hybridize with single-stranded DNA (ssDNA).[24–28]

During minus-strand synthesis, the RT degrades the RNA concomitantly with polymerization, although cleavages are not made as frequently as nucleotides are incorporated, leaving fragments of RNA still annealed to the nascent DNA.[29–32] Additional RT molecules further degrade the remaining fragments independently of polymerization.[30–39] RNA cleavage leads to the emergence of invasion sites, sections of ssDNA that are exposed for the second intact RNA to invade and hybridize.[27,28] Results obtained *in vitro* suggest that creation of the invasion site is the rate-limiting step of the invasion-mediated mechanism of strand transfer.[40] After invasion, the RNA–DNA hybrid must propagate to the 3′-terminus of the nascent DNA to drive a terminus transfer, which completes the template switch. Hybrid propagation can proceed by the successive base pairing of nascent DNA with the second RNA, known as branch migration. Heath and DeStefano demonstrated transfer-related branch migration in strand-exchange reactions in the absence of RT.[41]

Branch migration is one of two possible mechanisms of hybrid propagation. The other is a proximity-based mechanism. The proximity effect is achieved through an invasion upstream of the DNA 3′-terminus, which increases the local concentration of the second RNA template around the nascent DNA. The proximity effect can engender terminus transfer, as suggested by the work of Song *et al*.[42]

In a way similar to the proximity mechanism, nucleocapsid protein (NC) also stimulates annealing by increasing local concentrations of complementary nucleic acid by way of aggregation.[43–45] NC, a 55-aa product of gag gene expression and processing, has two zinc fingers that allow it to interact with chaperone nucleic acids, with a preference for single-stranded RNA.[43,46–48] NC not only promotes aggregation but also destabilizes weak secondary structures.[49–53] Accordingly, NC increases strand-transfer efficiency, in part through facilitating the invasion step.[47,48,54–58] Additionally, NC promotes strand exchange so long as the product shares a greater region of complementarity compared with the reactant.[41,51,52]

It has been reported that 3–30 strand-transfer events occur per genome per replication cycle.[59–63] During reverse transcription, as an RT extends the primer terminus farther away from the primer binding site (PBS), the polymerizing RT and assisting RTs cleave the RNA template, creating an ever-increasing number of potential invasion sites—that is, the number of potential invasion sites increases proportionally with the length of cDNA extension. This would predict that transfer efficiency at any position of primer extension would be proportional to the distance of synthesis from the primer to that position. However, Jetzt *et al*. reported that recombination efficiency across the length of the HIV-1 genome varied between regions but did not increase with distance from the PBS.[60] This result suggests that some factor limits efficiency of strand transfer despite increasing opportunities for invasion. The study by Jetzt *et al*. is consistent with the expectation that the farther the primer terminus is removed from an invasion site, the less likely the RNA–cDNA hybrid created by invasion can propagate quickly and efficiently enough to catch the DNA terminus and complete the transfer:[60] That is, efficiency by which hybrid propagation can contribute to transfer is expected to decrease substantially with distance. Considering the likelihood of limitations on the distances between invasion and terminus transfer and the limited number of transfer events, it is probable that transfer mechanisms are determined by local structures and conditions. The factors that determine hybrid propagation rate and efficiency have heretofore been largely unexplored.

Measurements of strand transfer made *in vitro* suggest that distances from invasion sites to points of terminus transfer can be separated by dozens of nucleotides.[28,40,64–66] However, each substrate system employed has had several potential sites of invasion, excluding precise measurement of the distance over which a specific invasion site can promote terminus transfer. Studies have investigated the influences of NC on strand-exchange reactions with a specific invasion site over shorter lengths, but the limitations of propagation distance with respect to specific invasion sites are undefined.[41,51,52] Here, we used specially designed RNA and DNA transfer substrates *in vitro* to determine how individual invasion sites contribute to the invasion-mediated mechanism of strand transfer, with specific focus on the limits and influences on the apparently crucial intermediate step of hybrid propagation. In particular, we investigated the roles of the RNase H activities of RT and the strand-exchange properties of NC.

Results

Our objectives were threefold: to design and use a reconstituted system able to test directly for the influence of a specific invasion site in strand transfer; to determine whether the hybrid propagation step of transfer is limited by distance; and to establish whether hybrid propagation is affected by the strand-exchange properties of NC and the RNase H activity of RT.

Pre-created invasion site substrates used in hybrid propagation experiments

Pre-created invasion site (PCIS) substrates have a single-stranded region that allows rapid, efficient acceptor invasion at a specific location.[40] The PCIS substrates used in this study were composed of a DNA primer annealed to either a DNA or an RNA donor template in which the primer had a 5′ overhang of 20 nt (Fig. 1). This region of the ssDNA primer is the PCIS and has a G/C content of 45% to promote invasion. Substrates are labeled −PCIS and +PCIS, indicating the absence and the presence, respectively, of the 20-nt 5′ overhang. An acceptor template, A_m, was designed to have full complementarity with the primer, including the region of the PCIS, with the exception of 3 nt that created a mismatch between the primer 3′-terminus and the acceptor template (Table 1). The mismatch was introduced to prevent polymerization on the acceptor should the primer exchange from the donor to the acceptor before initiation of synthesis on the donor. We observed that the 3-nt mismatch inhibited template-directed synthesis in reactions with primed acceptor and no donor (data not shown). A U33A base substitution was also introduced for the strand-exchange reactions described elsewhere (see Materials and Methods). The +PCIS substrate is designed to resemble the strand-transfer reaction intermediate just after creation of the invasion site.

The PCIS substrates offer unique advantages for characterizing the transfer mechanism. Comparing transfer efficiency from substrates having with those lacking the PCIS allows a confident determination of the role of invasion at that specific site on subsequent transfer. Since the substrates are designed such that the primer terminus must progress well downstream of the PCIS before transfer can occur, evidence that transfers initiate at the PCIS and complete later would provide the strongest model *in vitro* to date supporting the proposed invasion-mediated transfer mechanism.

Use of these substrates also facilitates assessment of the effects of two reaction components that we predicted to influence hybrid propagation and terminus transfer. The first is NC, which has been reported to promote strand exchange. The second is RT RNase H, which is anticipated to allow the initial DNA–RNA hybrid to expand by cutting the donor RNA (D_{RNA}) so as to destabilize its interaction with the cDNA. The effects of RNase H can be eliminated experimentally through the use of the E478Q mutant RT, which lacks RNase H function.

Effects of the PCIS and NC on transfer

We first questioned whether the presence of the PCIS influenced transfer. We used the primers $-PCIS_{20}$ and $+PCIS_{20}$, which were complementary with the last 20 nt of the 3′ end of the donor template and had 3-nt mismatch with the acceptor RNA, A_m, at nucleotide positions 18–20 (Table 1). Results indicated that the PCIS generally increased transfer efficiency (see Materials and Methods for determination of transfer efficiency) whether or not NC or RNase H was present (Fig. 2). The transfer efficiency of reactions with E478Q RT and no PCIS was a very low 0.6%, but it was significantly increased with the PCIS by as much as 6-fold to 3.6% (Fig. 2b and c; Table 2). Comparatively, the increase of transfer efficiency when NC and PCIS were combined in the presence of E478Q was approximately 19-fold to 11.4%.

We next asked whether NC could substitute for the PCIS. In a reaction with E478Q RT on a substrate without the PCIS, addition of NC increased the transfer efficiency by a mere 1.5-fold to 0.9%. Evidently, the PCIS had a more influential role in promoting strand transfer than NC when RT-RNase H activity was absent.

To further clarify the effects of PCIS and NC on strand transfer in the absence of RNase H, we repeated the previous reactions with wild-type (WT) RT and a DNA donor template instead of E478Q and an RNA donor template. The transfer efficiency for

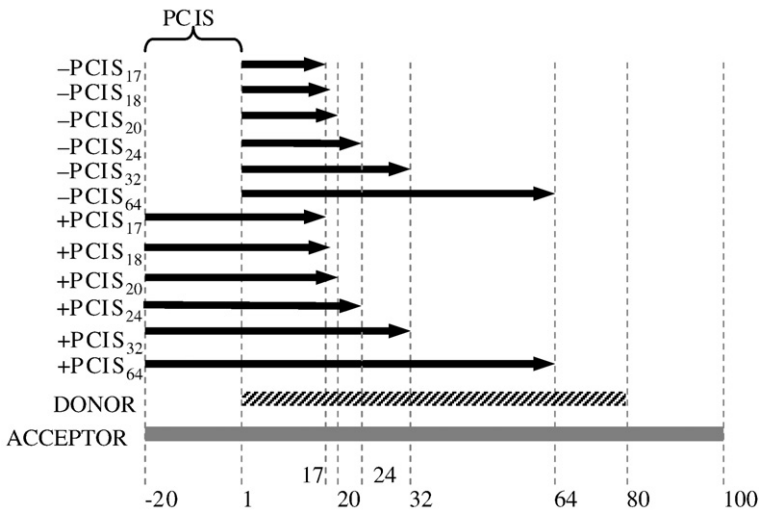

Fig. 1. Schematic of primers and templates used for PCIS experiments. The PCIS on selected substrates is indicated. Primer names contain (−) and (+) signs to indicate the absence and the presence, respectively, of the PCIS. The subscript number in the primer name indicates the length of primer that anneals with the donor template. Nucleotide numbering is indicated by dashed vertical lines and numbers. Black arrows represent the various DNA primers. The hatched line represents D_{RNA}. The continuous gray line represents the acceptor RNA.

Table 1. Primers (5′–3′) and acceptor and donor templates (3′–5′) used in the study

Name	Sequence	Length	PCIS
Primers			
$-PCIS_{17}$	TGGTAAACATTCTTGAG	17	−
$+PCIS_{17}$	CCGGTTCTATAACGGTATGATGGTAAACATTCTTGAG	37	+
$-PCIS_{18}$	TGGTAAACATTCTTGAGA	18	−
$+PCIS_{18}$	CCGGTTCTATAACGGTATGATGGTAAACATTCTTGAG$\overline{A}$	38	+
$-PCIS_{20}$	TGGTAAACATTCTTGAG$\overline{TG}$C	20	−
$+PCIS_{20}$	CCGGTTCTATAACGGTATGATGGTAAACATTCTTGAGTGC	40	+
$-PCIS_{24}$	TGGTAAACATTCTTGAGTGCTCGA	24	−
$+PCIS_{24}$	CCGGTTCTATAACGGTATGATGGTAAACATTCTTGAGTGCTCGA	44	+
$-PCIS_{32}$	TGGTAAACATTCTTGAGTGCTCGATCTGATGT	32	−
$+PCIS_{32}$	CCGGTTCTATAACGGTATGATGGTAAACATTCTTGAGTGCTCGATCTGATGT	52	+
$-PCIS_{64}$	TGGTAAACATTCTTGAGTGCTCGATCTGATGTAAGCTTAGACTTGTACTGCGATGTGTAGTGAG	64	−
$+PCIS_{64}$	CCGGTTCTATAACGGTATGATGGTAAACATTCTTGAGTGCTCGATCTGATGTAAGCTTAGACTTGTACTGCGATGTGTAGTGAG	84	+
Acceptors			
A_m	GGCCAAGAUAUUGCCAUACUACCAUUUGUAAGAACUCUUCAGCUAGACUACAAUCGAAUCUGAACAUGACGCUACACAUCACUC**UGCAUAUGAGCAUCCUAGC**CUCGAGGUUAAGCGGG	119	+
A_{17}	GGCCAAGAUAUUGCCAUACUACCAUUUGUAAGAACUC$\overline{UCG}$AGCUAGACUACA$\overline{U}$UCGAAUCUGAACAUGACGCUACACAUCACUC**UGCAUAUGAGCAUCCUAGC**CUCGAGGUUAAGCGGG	119	+
A_{24}	GGCCAAGAUAUUGCCAUACUACCAUUUGUAAGAACUC$\overline{A}$CGAGCUUGACUACAUUCGAAUCUGAACAUGACGCUACACAUCACUC**UGCAUAUGAGCAUCCUAGC**CUCGAGGUUAAGCGGG	119	+
A_{32}	GGCCAAGAUAUUGCCAUACUACCAUUUGUAAGAACUCACGAGCU$\overline{A}$GACUACA$\overline{A}$UCGAAUCUGAACAUGACGCUACACAUCACUC**UGCAUAUGAGCAUCCUAGC**CUCGAGGUUAAGCGGG	119	+
A_{64}	GGCCAAGAUAUUGCCAUACUACCAUUUGUAAGAACUCACGAGCUAGACUACA$\overline{U}$UCGAAUCUGAACAUGACGCUACACAUCACUC**UGCAUATGAGCAUCCUAGC**CUCGAGGUUAAGCGGG	119	+
Donors			
D_{RNA}	ACCAUUUGUAAGAACUCACGAGCUAGACUACAUUCGAAUCUGAACAUGACGCUACACAUCACUC ... ... CUCGAGGUUAA GCGGG	80	−
D_{DNA}	ACCATTTGTAAGAACTCACGAGCTAGACTACATTCGAATCTGAACATGACGCTACACATCACTC ... ... CTCGAGGTTAAGCGGG	80	−

Primers are named $-PCIS_{\#\#}$ or $+PCIS_{\#\#}$, with the (−) and (+) signs indicating the absence and the presence, respectively, of the invasion site and subscript numbers indicating the length of the primer that anneals with the donor template. Acceptors are named $A_{\#\#}$, with the numbers corresponding to the hybrid propagation distance. The donor templates are named D_{RNA} or D_{DNA}, indicating whether the donor template is RNA or DNA. Sequences are aligned for homology or complementarity. Sequences in boldface indicate the nonhomologous sequence inserted in the acceptor to prevent detection of end-transfer products. Underlined nucleotides differ from the donor template.

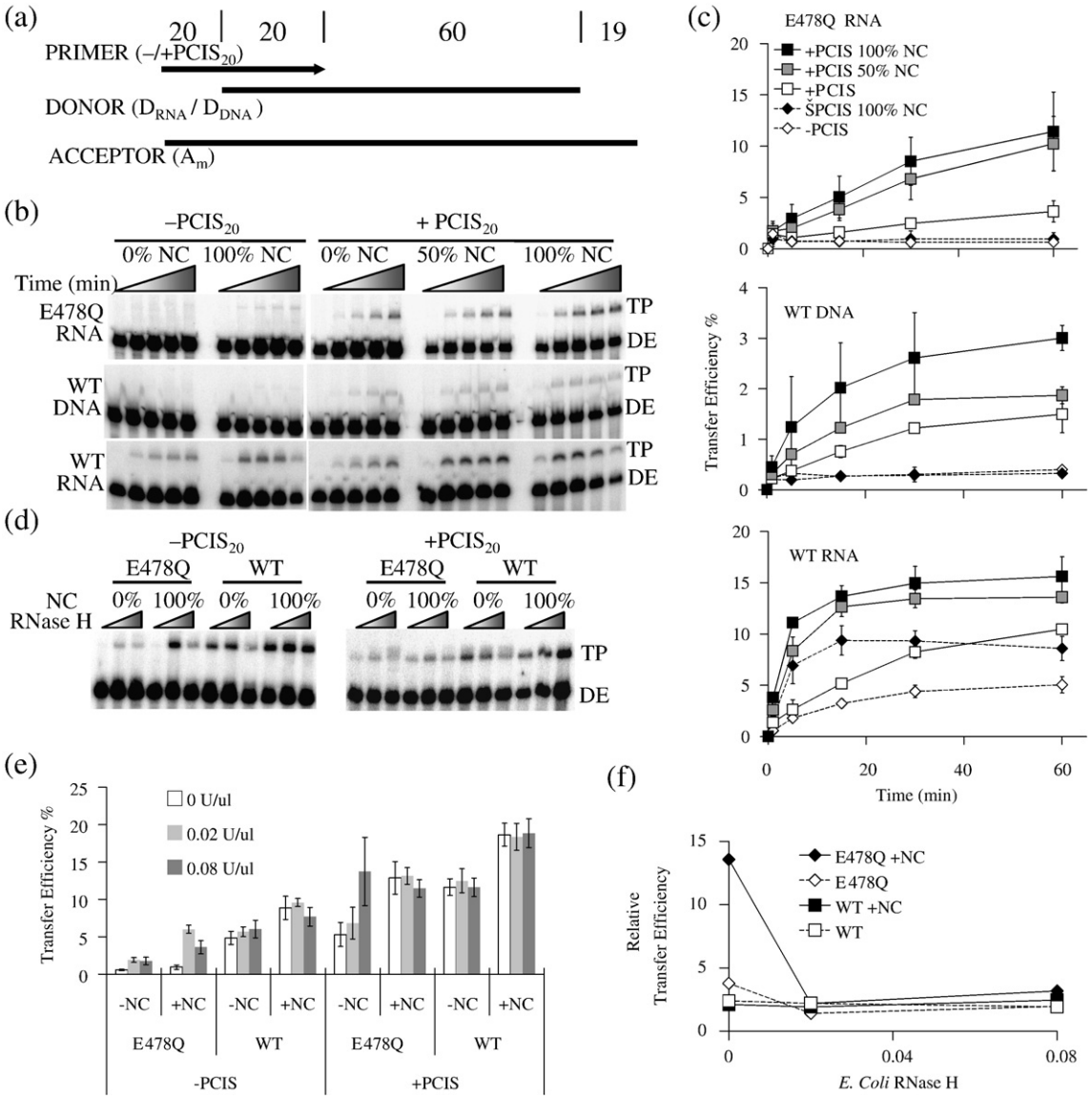

Fig. 2. PCIS-mediated strand transfer. (a) 5′-Radiolabeled DNA primers were heat annealed to either RNA or DNA donors. Reactions were initiated with the addition of Mg^{2+}, deoxy-NTPs, and the acceptor RNA, A_m. $-PCIS_{20}$ indicates experiments with radiolabeled DNA primers lacking the PCIS, while $+PCIS_{20}$ indicates the presence of the PCIS. The numbers above the templates indicate the length in nucleotides of each segment. (b) Effects of the PCIS, NC, and RT-RNase H activity on hybrid propagation. Gel images of E478Q RT with an RNA donor template, WT RT with a DNA donor template, and WT RT with an RNA donor template. (c) Graph symbols defined in E478Q RNA are the same for WT DNA and WT RNA. (d) *E. coli* RNase H titration in PCIS strand-transfer reactions. RNase H is titrated from 0 U/μl to 0.02 and 0.08 U/μl. (e) Graph of transfer efficiencies calculated from PCIS strand-transfer reactions. White bars indicate reactions without exogenous *E. coli* RNase H. Light gray bars indicate reactions with 0.02 U/μl of *E. coli* RNase H. Dark gray bars indicate reactions with 0.08 U/μl of *E. coli* RNase H. (f) Graph of the relative transfer efficiency (RTE) of PCIS reactions. RTE is the ratio of transfer efficiencies with to those without the PCIS (see Materials and Methods).

these reactions without a PCIS and an NC was 0.4% (Fig. 2b and c). Much like the E478Q reactions, the low transfer efficiency of the DNA donor reactions was increased with the addition of a PCIS by 3.8-fold to 1.5% (Table 2). Again, NC had little effect on strand transfer without the PCIS, altering the transfer efficiency only to 0.3%, but stimulated transfer by 7.5-fold to 3.0% when the PCIS was present. While the trend of the results with WT RT and a DNA donor is similar to E478Q RT and an RNA donor, the transfer efficiencies were generally lower, presumably because of the characteristics of the DNA–DNA primer–donor helix. Results with both reaction systems support the conclusion that the PCIS is critical for efficient transfer for a template system in which RNase H does not cut the donor template. Moreover, both systems indicate that NC functions primarily through facilitating the role of the PCIS in transfer. Very likely, this includes promoting acceptor–cDNA primer interaction at

Table 2. Fold increase of strand-transfer efficiency in PCIS substrates with variables

		$-PCIS_{20}$		$+PCIS_{20}$	
RT	Donor	0% NC	100% NC	0% NC	100% NC
E478Q	D_{RNA}	1	1.5	6	19
WT	D_{DNA}	1	0.8	3.8	7.5
WT	D_{RNA}	1	1.7	2.1	3.1

All results are normalized to −PCIS 0% NC experimental results. −PCIS indicates experiments performed with DNA primers lacking the PCIS, while +PCIS indicates experiments performed with those having the PCIS.

the PCIS and subsequent strand exchange to complete transfer. This assumption is in agreement with evidence showing that substrates with a PCIS have an increased rate of strand transfer with increasing acceptor concentration and that NC enhances the formation of stable acceptor–primer hybrids at the PCIS.[40,41]

Effects of RNase H on transfer

To examine the influence of RNase H on strand transfer with the PCIS substrates, we repeated the above experiments using WT RT with the RNA donor substrates. Even without the PCIS and NC, the strand-transfer reactions yielded a distinctly higher 5.1% efficiency with RNase H (Fig. 2b and c). With the introduction of the invasion site, transfer increased by 2-fold to 10.5%. Without the PCIS, NC increased transfer efficiency by 1.7-fold to 8.6%. In combination, the PCIS and NC stimulated transfer efficiency by 3-fold to 15.6%. Clearly, the introduction of RNase H activity markedly reduced the percentage of impact of both the stimulation by the PCIS and combined PCIS and NC stimulation of strand transfer. The percentage of effect of NC alone remained similar to results without RNase H, however. A reasonable conclusion is that cuts made by the RT RNase H partially substitute for the PCIS and NC. The RNase H cuts are likely to create alternative invasion sites and weaken the donor–primer interaction to reduce the energy barrier to strand exchange from the PCIS and every invasion site, similar to the effects of NC.

A second approach to examining the effects of RNase H activity on invasion-mediated strand transfer was to repeat the previously described E478Q or WT RT reactions, but with exogenous RNase H activity in the form of *Escherichia coli* RNase H. The addition of exogenous RNase H (0.08 U/μl) increased transfer efficiency with substrates lacking the PCIS from 0.6% to 1.8% (Fig. 2d and e). In reactions with the PCIS, exogenous RNase H increased transfer efficiency from 5.3% to 6.8% and 13.8% for 0.02 and 0.08 U/μl, respectively. Upon addition of NC, transfer efficiency without the PCIS was increased from 0.9% to a significant 6.0% and 3.6% for 0.02 and 0.08 U/μl, respectively. Addition of NC to reactions with the PCIS slightly altered the transfer efficiency from 12.9% to 13.1% and 11.5% for 0.02 and 0.08 U/μl, respectively. The −PCIS/+PCIS ratios for E478Q reactions lacking exogenous RNase H were 3.8 without NC and 13.6 with NC (Fig. 2f). The addition of exogenous RNase H dropped the −PCIS/+PCIS transfer ratio to near the levels seen with WT RT. Inclusion of exogenous RNase H, as with use of WT RT, reduced the influence of the PCIS in strand-transfer reactions. Interestingly, NC stimulated transfer efficiency in reactions lacking the PCIS only when RNase H was present, either exogenous or with WT RT, perhaps through enhancing interactions between the acceptor and the primer at invasion sites created during the reactions by RNase H activity. We suspect that the PCIS was the more commonly used invasion site in WT RT reactions as compared with invasion sites created by RNase H activity because there was less stimulation by NC in exogenous RNase H-containing reactions with WT than with E478Q.

Most permutations of reaction conditions with E478Q RT and *E. coli* RNase H did not yield transfer efficiencies similar to WT levels. These results suggest that there is some advantage to transfer efficiency of combining polymerization and RNase H functions in the same molecule or that the ratio of the rates of polymerase to RNase H activity is critical for efficient strand transfer.

Distance effects on hybrid propagation

As discussed above, the fact that recombination in HIV-1 does not increase with synthesis distance from the PBS suggests that the invasion site can affect transfer over only a limited distance. To address this issue mechanistically, we tested the distance-related restrictions on hybrid propagation by measuring the efficiency of template strand exchange over time, as occurs during the transfer reaction, using a substrate design that simulates primer elongation to a specific distance from the PCIS. The approach was to construct substrates in which the length of the primer hybridized to the D_{RNA} was altered from the original 20 nt to 17, 24, 32, and 64 nt (Figs. 3a, 4a, 5a, and 6a). Each acceptor RNA to be used was constructed with a base substitution, compared with the D_{RNA} sequence, 1 nt after the 3′ terminus of the tested primer. Time-dependent completion of strand exchange was assessed by the efficiency of incorporation of the nucleotide specific for base pairing to the acceptor RNA. This was accomplished by having only the appropriate deoxy-NTP for incorporation after exchange present as a reactant. Each propagation distance was measured with acceptor templates that either contained the 3-nt mismatch or were perfectly complementary with the primer to assess the influence of the 3-nt mismatch in strand-transfer reactions with the primers $-PCIS_{20}$ and $+PCIS_{20}$ in Fig. 2.

For nucleotide incorporation to represent the strand-exchange rate, incorporation must be fast relative to strand exchange. To measure the rate of

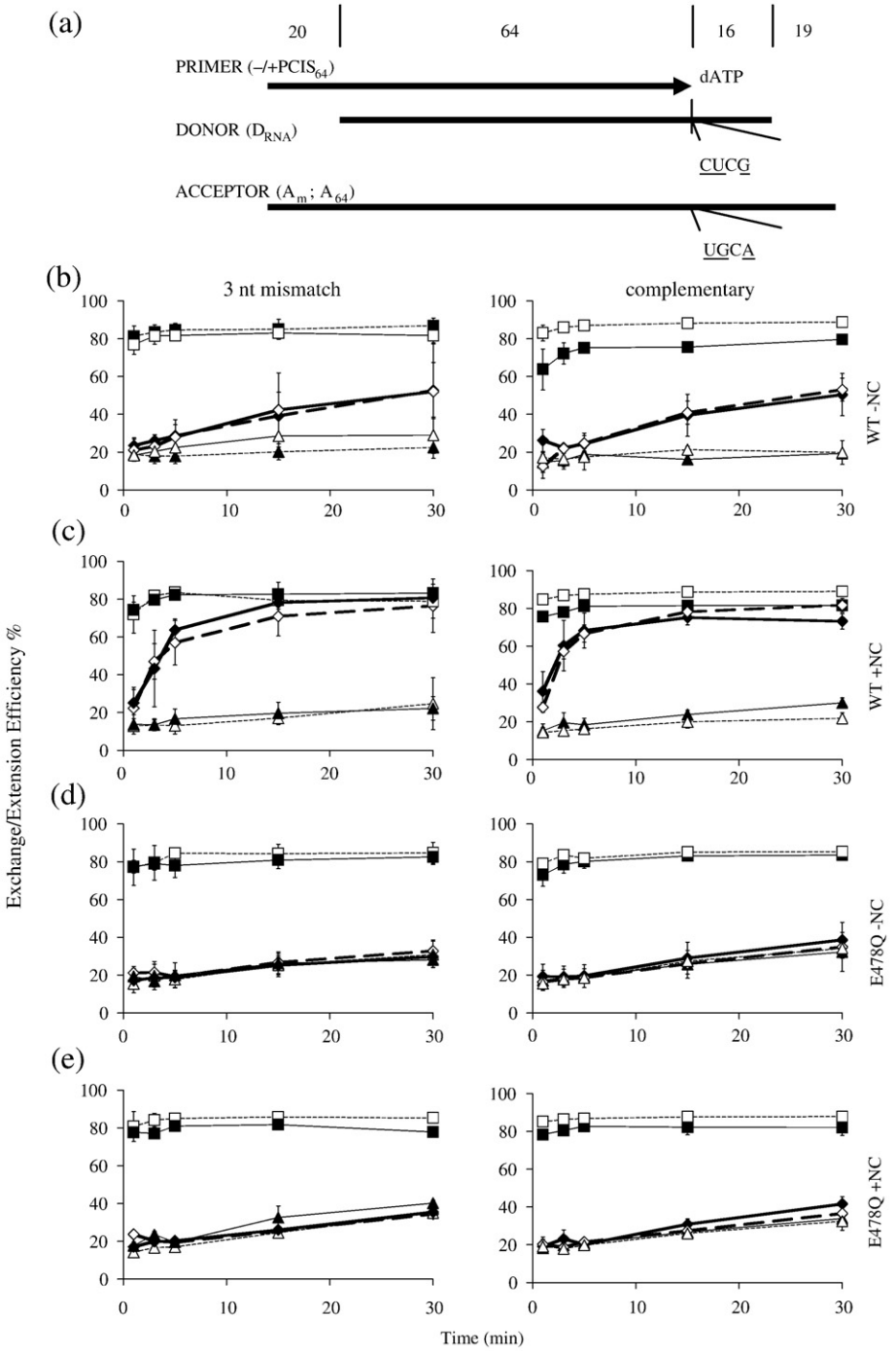

Fig. 3. Acceptor–primer hybrid propagation through 64 nt of pre-annealed primer–donor hybrid. (a) $-PCIS_{64}/+PCIS_{64}$, D_{RNA}, and acceptor RNAs indicate the primers and templates used. Only deoxy-ATP was used in the reactions. Donor and acceptor sequences immediately following the primer 3′-terminus are shown, and nonhomologous bases are underlined. The numbers above the templates indicate the nucleotide distances for various segments of the substrates. (b–e) "3-nt mismatch" indicates a mismatch between the primer DNA and the acceptor RNA, A_m, at nucleotide positions 18–20. "Complementary" indicates that the primer and acceptor are fully complementary. Dashed lines and white symbols represent transfer efficiency for −PCIS reactions, while continuous lines and black symbols represent that for +PCIS reactions. Squares indicate extension efficiencies with primed acceptor only. Diamonds indicate strand-exchange efficiencies with primed donor and free acceptor. Triangles indicate extension efficiencies with primed donor only. (b) Reactions with WT RT and no NC. (c) Reactions with WT RT and 100% NC coating. (d) Reactions with E478Q RT and no NC. (e) Reactions with E478Q RT and 100% NC coating.

incorporation, we performed control reactions with the primer pre-annealed to the acceptor RNA. A comparison of exchange rate with extension rate on the acceptor demonstrated that nucleotide incorporation was not determining the rate of exchange plus incorporation. Therefore, in the actual reaction,

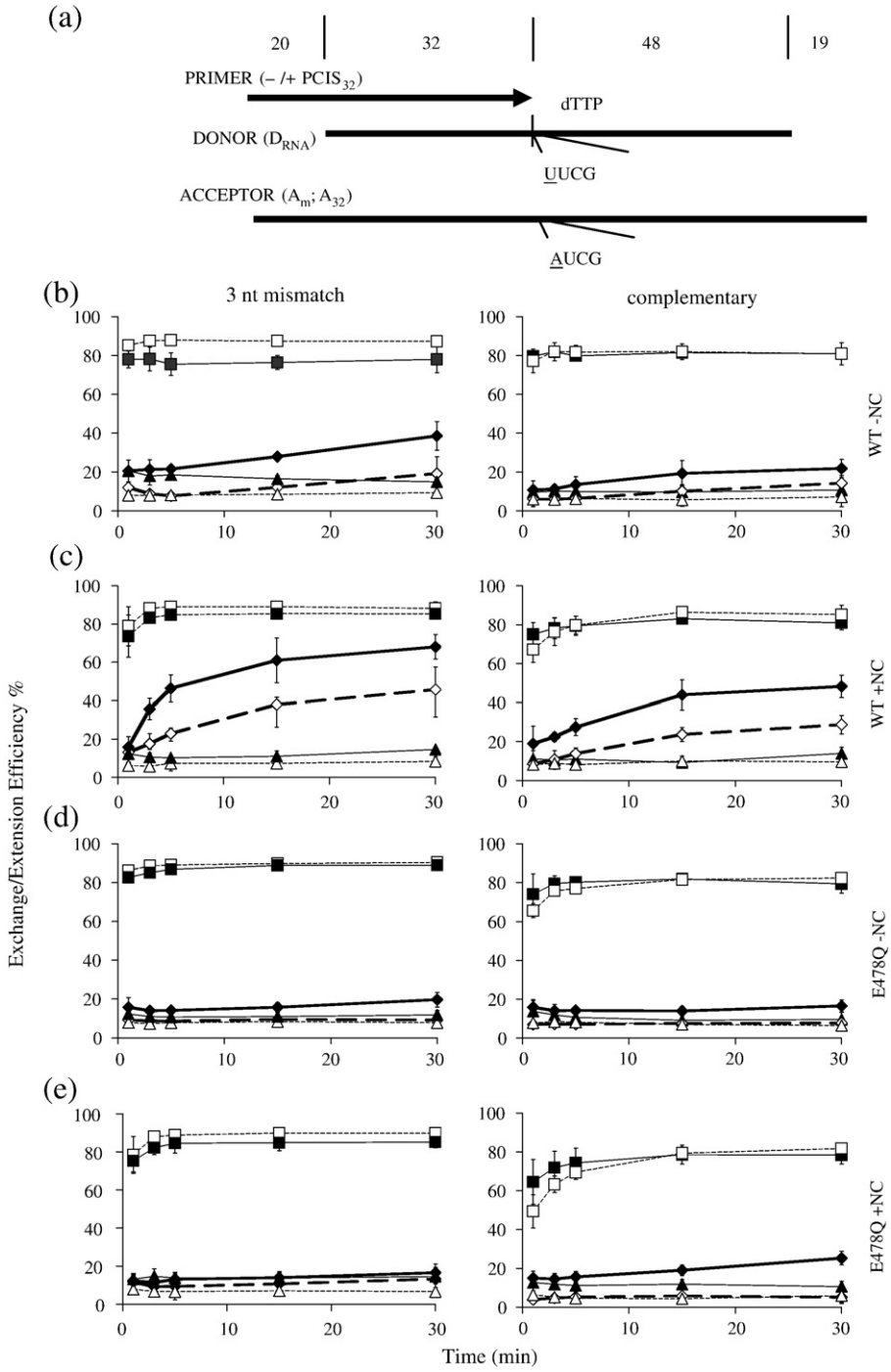

Fig. 4. Acceptor–primer hybrid propagation through 32 nt of pre-annealed primer–donor hybrid. Only deoxy-TTP was used in the reactions. For symbol designations and reaction conditions, see the legend to Fig. 3.

nucleotide incorporation was an appropriate quantitative indicator of strand-exchange rate. Reactions were also performed with the primer pre-annealed to the donor template and no acceptor template present to control for non-template-directed deoxy-NTP incorporation. Exchange efficiencies rising above this background control are therefore a result of strand exchange, not misincorporation. The efficiencies of incorporation on the donor and acceptor templates are represented along with the exchange efficiency on graphical axes of exchange/extension efficiency in Figs. 3–6 so that the three values can be directly compared.

Reactions were performed using substrates either having or lacking the PCIS. This allowed us to quantitate the effect of the PCIS on the rate of exchange of the primer from the donor to the acceptor template. For example, some reactions with a PCIS and E478Q RT show clear evidence of strand exchange by branch migration, specifically deriving

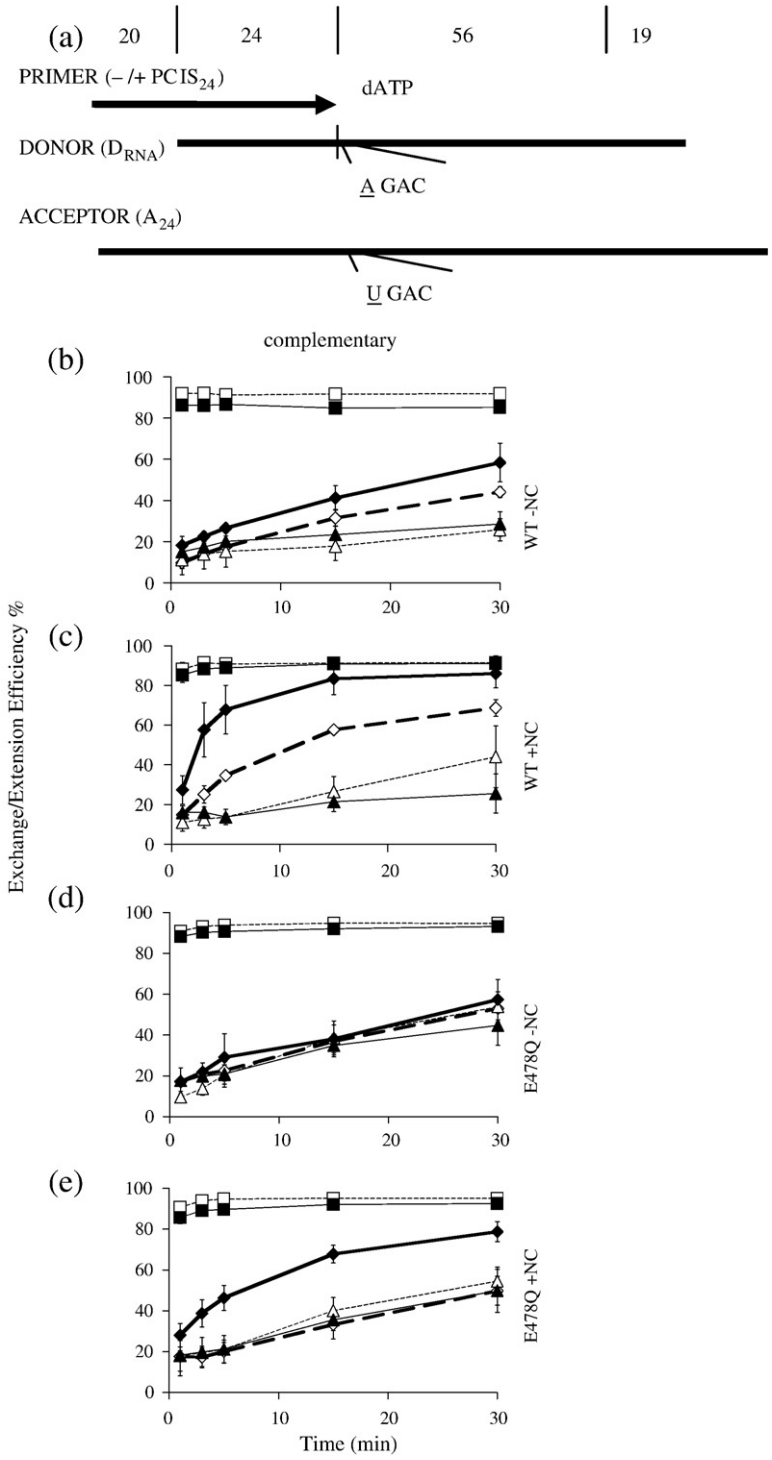

Fig. 5. Acceptor–primer hybrid propagation through 24 nt of pre-annealed primer–donor hybrid. Only deoxy-ATP was used in the reactions. For symbol designations and reaction conditions, see the legend to Fig. 3. Only results from experiments with full complementarity between acceptor and primer are shown.

from invasion at the PCIS, not observed in the same reactions lacking a PCIS. Each distance has revealed unique distance-related characteristics of the hybrid propagation step.

Characteristics of each propagation distance

Reactions with the primer sets $-PCIS_{64}$ and $+PCIS_{64}$ showed that at the longest propagation distance tested, 64 nt, transfer efficiency with E478Q RT remained at the background, even in the presence of the PCIS and NC (Fig. 3c and e). Yet, with WT RT, although the PCIS alone had no distinguishable influence on transfer efficiency, addition of NC to the PCIS substrate increased the transfer rate and efficiency (Fig. 3b and d). These results show that RNase H activity was required for efficient transfer when a distance of 64 nt separated the invasion site and primer terminus. Moreover, NC influenced strand transfer in PCIS reactions only when RNase H activity was present. These observations imply that once the

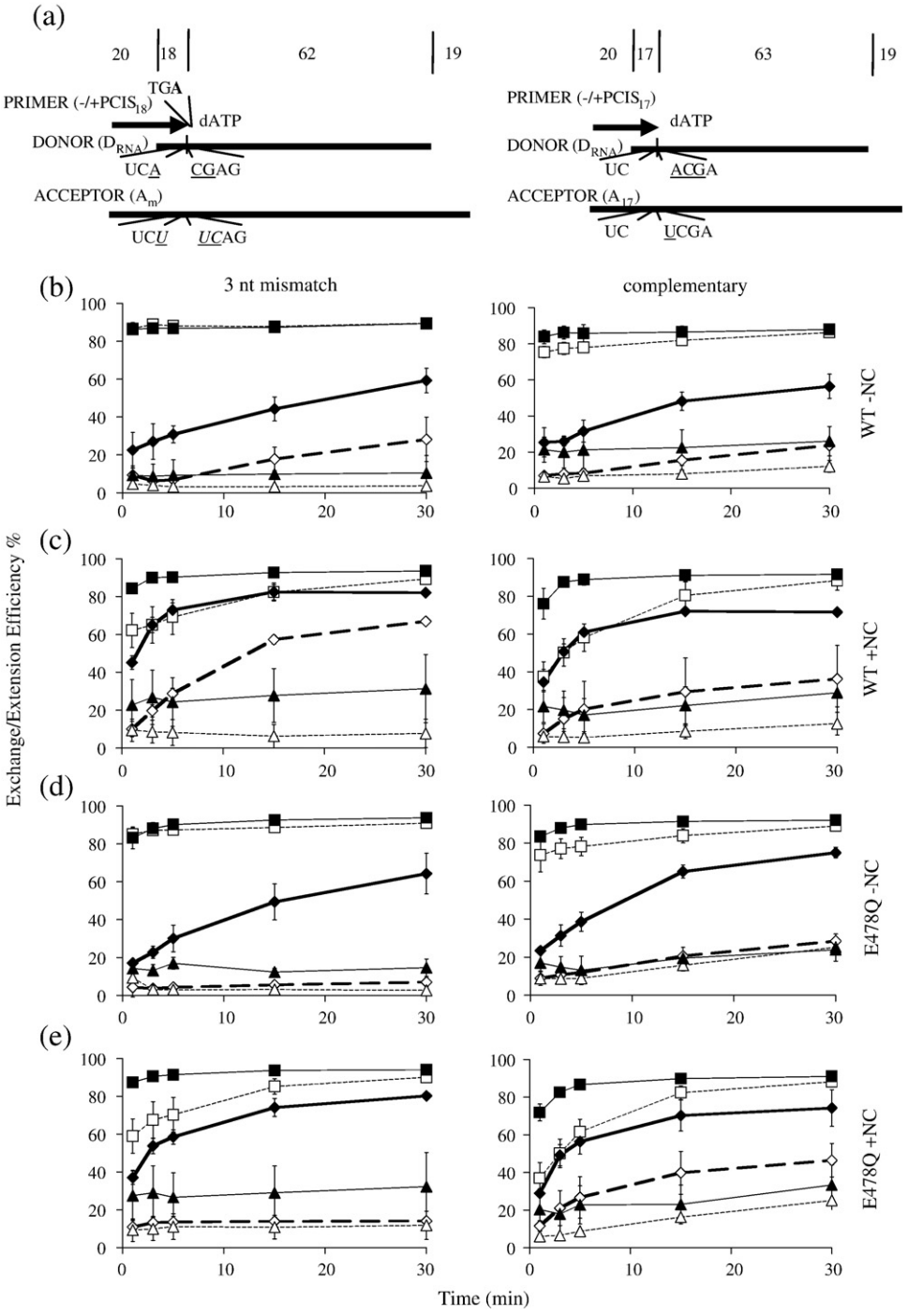

Fig. 6. Acceptor–primer hybrid propagation through 17 nt of pre-annealed primer–donor hybrid. Only deoxy-ATP was used in the reactions. The 3-nt mismatch in A_m is italicized, and the $-PCIS_{18}/+PCIS_{18}$ mismatch with the donor is in boldface. For all other symbol designations and reaction conditions, see the legend to Fig. 3.

hybrid propagation length reaches approximately 64 nt, hybrid propagation over the full distance rarely occurs, and that creation of new invasion sites closer to the primer 3′-terminus is necessary for efficient strand transfer. The differences between reactions with and those without the primer–acceptor 3-nt mismatch are minimal, which suggests that the mismatch had little influence on strand exchange over 64 nt.

Reactions with $-PCIS_{32}$ and $+PCIS_{32}$ revealed the distance, approximately 32 nt, at which the PCIS moderately influenced strand-transfer efficiency, but only with WT RT. Just as with the 64-nt propagation distance, strand exchange at the 32-nt distance with the E478Q RT remained at the background, even with the PCIS and NC for reactions with the 3-nt mismatch (Fig. 4c and e). Complementary reactions without the mismatch displayed a moderate rise of

strand exchange above background with PICS, NC, and E478Q. This difference is likely due to the altered acceptor structure, although it is possible that there is inhibition of branch migration beyond the 3-nt mismatch. Our purpose for comparing strand-exchange efficiency with and that without the primer–acceptor mismatch was to determine whether the mismatch inhibited hybrid propagation in the strand-transfer reactions. It appears that a mismatched region of three nucleotides has little effect on strand exchange across a distance of 32 nt and probably did not significantly influence the strand-transfer reactions.

Similar to the 64-nt reactions, NC increased exchange efficiency with WT RT; however, unlike the longer distance, at 32 nt, the +PCIS reactions had a higher transfer efficiency than the −PCIS reactions (Fig. 4b and d). Exchange efficiencies with the 3-nt mismatched acceptor templates, WT RT but no NC, were 39% and 20% for $+PCIS_{32}$ and $-PCIS_{32}$, respectively. For the similar reactions with complementary primer and acceptor, exchange efficiencies were 22% and 14% for $+PCIS_{32}$ and $-PCIS_{32}$, respectively. Strikingly, exchange efficiencies with NC achieved the high values of 70% and 45% for $+PCIS_{32}$ and $-PCIS_{32}$, respectively. For similar reactions with complementary primer and acceptor, exchange efficiencies were 48% and 29% for $+PCIS_{32}$ and $-PCIS_{32}$, respectively. Clearly, the PCIS was more influential in strand exchange with the 32-nt distance than with the 64-nt hybrid propagation distance. Results with E478Q RT revealed minimal influence of the PCIS on exchange efficiency with the aid of NC. Therefore, RNase H activity still greatly facilitated efficient exchange with the 32-nt propagation distance but was not absolutely required. At 32 nt, branch migration alone, although highly inefficient, could be a pathway in the mechanism of strand transfer.

Results from strand-exchange experiments with the primers $-PCIS_{24}$ and $+PCIS_{24}$ reveal that branch migration did not occur over a distance of 24 nt without RNase H activity and the PCIS (Fig. 5). NC could stimulate efficient branch migration without RNase H activity so long as the PCIS was present. Upon introduction of RNase H activity with the WT RT, exchange efficiency rose above the background even without the PCIS, although the PCIS significantly increased transfer efficiency in the presence of NC. A comparison of the results from the 32-nt strand-exchange experiments with those from the 24-nt distance experiments implied that NC increasingly promotes invasion-mediated branch migration with decreasing distances of hybrid propagation.

It was not possible to assess strand exchange over 24 nt with mismatched substrates because nucleotide incorporation from the primer on the acceptor template was approximately 1 order of magnitude slower than in all other exchange reactions (data not shown). This was likely because the 3-nt mismatch at positions 18–20 destabilized primer–acceptor annealing at positions 21–24, which inhibited rapid extension at position 25.

The primers $-PCIS_{17}$, $+PCIS_{17}$, $-PCIS_{18}$, and $+PCIS_{18}$ are all complementary with the last 17 nt of the D_{RNA} 3′ end (Fig. 1; Table 1). The primer pair $-PCIS_{17}/+PCIS_{17}$ is complementary up to position 17 on A_{17}, and the pair $-PCIS_{18}/+PCIS_{18}$ is complementary up to position 18 on A_m (Figs. 1 and 6a; Table 1). These are 17-nt exchange reactions because the length of the donor that must be displaced by the hybrid propagation reaction is the same for both substrates. The 17-nt exchange results revealed that strand transfer can occur by strand exchange alone even with E478Q. Even with this substrate, however, RNase H increases transfer efficiency. E478Q reactions had an exchange efficiency significantly above the background only when the PCIS was present. NC increased the transfer efficiency of only +PCIS reactions with the 3-nt mismatched acceptor Am2 and both +PCIS and −PCIS reactions with the complementary acceptor Am9 (Fig. 6c and e). With WT RT, PCIS-mediated reactions were more efficient than −PCIS reactions, and NC increased the transfer efficiency of both −PCIS and +PCIS reactions (Fig. 6b and d). Differences between reactions with the acceptors Am2 and Am9 are likely from differences in template structures since the primers are entirely complementary to their respective acceptors. Results suggest that when the hybrid needs to propagate only 17 nt, the approximate distance separating the RNase H and polymerase domains of RT, strand exchange is facile, even in the absence of RNase H, but always requires the PCIS.

Discussion

The proposed invasion mechanism for strand transfer in retroviruses such as HIV-1 involves the steps of acceptor invasion, RNA–DNA hybrid propagation, and ultimate terminus transfer of the DNA from the donor to the acceptor RNA template. Depending on the relative rates of cDNA synthesis and hybrid propagation, positions of invasion and terminus transfer could be separated by considerable distances. Primer extension from the PBS during reverse transcription *in vivo* is expected to create progressively more potential invasion sites for transfer. However, transfer events previously measured across the HIV-1 genome showed no significant increase in transfer efficiency the farther the DNA 3′-terminus was extended from the PBS.[60] These results imply a distance-related limitation on efficient invasion-mediated strand transfer. Here, we report the development and use of a model system *in vitro* designed to measure the distance over which a specific invasion site can promote strand transfer, as well as the effects of substrate structure and protein components of the reaction. The strand-exchange step of transfer was previously shown to require a single-stranded region in the primer–donor substrate to act as a site for invasion by the acceptor.[40,41,52,66–69] Heath and DeStefano examined the effects of NC, invasion site size, and

primer–acceptor complementarity on the strand-exchange reaction. It was observed that longer invasion sites generally lead to higher transfer efficiency and that strand exchange could propagate through 25 nt with as little as 10 nt for invasion.[41] Also, NC was demonstrated to inhibit strand exchange for acceptor–primer substrates with mismatches in the invasion region and promote the exchange reaction by stimulating the interaction of complementary acceptor and primer sequences.[41] We have expanded on these results to present a comprehensive biochemical analysis of the strand-transfer reaction. It provides the best evidence so far that strand transfers actually occur by a multi-step invasion-mediated mechanism. The force of evidence comes from the observation that the presence of a specific PCIS increased the efficiency of a primer terminus transfer occurring well downstream with respect to synthesis. Moreover, the analysis defined distance limitations on invasion-initiated hybrid propagation leading to transfer and revealed the significance of combinations of a PCIS, NC, and RT RNase H on efficiency of transfer.

A comparison of results of RT-mediated transfer assays using substrates having or lacking a PCIS and without NC or RNase H clearly demonstrated the need for an invasion site to allow transfer. The experiments revealed that, whether or not NC is present, it is essential to have an invasion site for efficient primer–acceptor branch migration through a stable primer–donor hybrid. This suggests that the acceptor template simply cannot invade a fully double-stranded primer–donor substrate. Substrates with the PCIS allow some transfer, which is greatly enhanced by the presence of NC. In view of the well-known strand-exchange properties of NC,[43,70] it is logical to conclude that NC promotes both a stable initial interaction of the acceptor with the PCIS and an exchange of the donor and acceptor strands on the cDNA primer. This conclusion is fully consistent with earlier observations of NC stimulation of strand exchange.[41,43,51]

Reactions using WT RT instead of the RNase H-deficient E478Q mutant RT add an additional level of complexity. RNase H-containing RT, in the presence of NC, considerably increases transfer efficiency on substrates having and those lacking the PCIS. A reasonable interpretation is that the RNase H creates additional sites where the acceptor can invade. These would be generated throughout the D_{RNA}–cDNA hybrid region irrespective of the initial presence of a PCIS. Indeed, previous studies have shown that RNase H activity does promote initiation of strand transfer by creating invasion sites.[2,25,26,28,40,66–69,71]

We envision that the ability of the RNase H to make cuts in the hybrid region could result in additional phenomena. One possibility is that cuts in the donor template in the hybrid region would destabilize cDNA–donor helical stability. This would allow a cDNA–acceptor interaction at the PCIS to propagate more rapidly into the cDNA–donor region. However, if this were the primary effect of RNase H, we would expect that the relative amount of transfer observed would increase for substrates having *versus* those lacking a PCIS. In fact, the relative effectiveness of the PCIS is lessened by the presence of RNase H.

Moreover, the presence of both the PCIS and RNase H might promote transfer by an "acceptor proximity mechanism." In this process, the acceptor would initially interact with the PCIS. This interaction would raise the local acceptor concentration at downstream sites of RNase H cleavage. The proximity of the acceptor to these sites would promote additional interactions that would result in facile exchange of the acceptor for the donor. However, this mechanism would predict a greater relative effectiveness of substrates with the PCIS, which was not seen. While the destabilization and proximity effects are likely to make some contribution to transfer, the major effect of the RNase H appears to be the creation of additional invasion sites that can be used in addition to the PCIS.

Although RNase H reduced the impact of the PCIS on strand transfer, both NC and the PCIS still increased transfer efficiency in reactions with WT RT, and they were more effective at stimulating transfer in combination than separately. The stimulation by the PCIS and NC indicates that the branch migration or proximity mechanisms are still occurring in the presence of WT RT. Therefore, in the presence of the PCIS, NC, and RNase H, several transfer mechanisms collaborate to produce maximum transfer product.

If the primary effect of the presence of RNase H is to create usable invasion sites, the fact that RNase H greatly reduces the impact of the PCIS indicates that invasion sites closer to the DNA primer terminus are much more effective than farther invasion sites. It would follow that the effectiveness of the PCIS at promoting transfers falls off precipitously with the distance between the PCIS and the DNA primer terminus. This means that most transfers that occur by an invasion mechanism, employing branch migration or acceptor proximity, propagate over a relatively short distance. While NC appears to facilitate branch migration, lengthening the effective range of an invasion site, the ultimate range must be confined. The effect of continuous RNase H activity would be to create a series of invasion sites from which transfers can initiate. This would produce hotspots of recombination across the HIV-1 genome but no increase of recombination with increasing distance from the PBS. In fact, this is exactly what has been observed *in vivo*.[60]

To better define the distance limitations on hybrid propagation in strand transfer, we performed strand-exchange experiments with substrates in which the length of the primer–donor hybrid was progressively altered. Each of the lengths, 17, 24, 32, and 64 nt, revealed valuable insights into the hybrid propagation mechanism. Exchange over the short distance of 17 nt occurred efficiently without RNase H but was still accelerated by the presence of RNA cleavage. Without RNase H, the PCIS was essential

for exchange. Even with RNase H, the PCIS had a positive influence. As discussed above, the ability of RNA cleavage to modestly accelerate branch migration might have been masked in the transfer experiments by the more dominant phenomenon of invasion site creation. Overall, results from reactions with the 17-nt duplex revealed that continuous migration of uncut branches is likely the dominant means of connecting an initial invasion with a successful primer terminus transfer (Fig. 7).

Branch migration through 24 nt of uncut strands was only efficient with the assistance of NC, and when the 3′-terminus and the PCIS were separated by 32 nt, migration of uncut strands was practically ineffective for strand exchange. This conclusion is based on the requirement for NC to rescue transfer in the presence of E478Q RT at 24 nt and the limited ability of NC to rescue transfer at 32 nt. In reactions with WT RT, the PCIS and NC both had a positive effect on the exchange reaction. This outcome suggests two possible mechanisms, discussed above, by which the contribution of the PCIS to strand exchange requires RNase H cleavage. Either the RNase H weakens D_{RNA}–cDNA interactions so that there can be branch migration of the initial PCIS–acceptor hybrid or the RNase H cleavage sites provide secondary points of acceptor interaction by proximity, after the initial PCIS–acceptor hybrid formation. This conclusion is consistent with our results showing that the presence of RNase H significantly improves transfer efficiency on a substrate with a PCIS.

As expected, the combination of E478Q RT and NC remained ineffective at promoting strand exchange when the PCIS and primer terminus were separated by 64 nt. However, exchange remained possible with WT RT and was promoted by NC. The notable feature of exchange reactions with this substrate is that there is no significant influence of the PCIS. Evidently, exchange proceeds completely from invasions initiated at RNase H cleavage sites beyond the PCIS (Fig. 7). Therefore, the 64-nt separation represents a distance completely beyond the range of hybrid propagation for strand transfer by any mechanism.

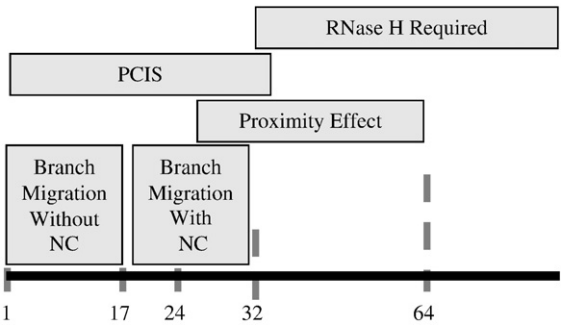

Fig. 7. Distances of mechanisms and influences of hybrid propagation. Vertical dashed lines and numbers indicate the distances in nucleotides. The numbering begins with the first nucleotide following the invasion site.

Based on our observations, we propose that the hybrid propagation step of strand transfer can proceed effectively by branch migration of intact RNA strands up to a distance of 32 nt, at least with the help of NC. At distances beyond this, RNase H cleavage of the donor strand is required. With RNase H, a specific invasion site can contribute to transfer to a distance of between 32 and 64 nt. Current results show branch migration occurring efficiently at 17 nt, less efficiently at 24 nt, and nearly nonexistentially at 32 nt. Yet, since there is a significant influence of the PCIS at 32 nt, we suspect that a combination of proximity effect and branch migration occurs across a hybrid propagation range of 24 nt to a position less than 64 nt. Therefore, we propose that transfers beyond 18–24 nt occur either by an acceptor proximity mechanism or by branch migration promoted by cleavages that weaken the donor–cDNA helical stability. This is consistent with previous results demonstrating efficient strand transfer through a proximity mechanism at a distance of approximately 40 nt although branch migration is not fully excluded since there is a possibility for strand exchange at the donor 5′ end, which shares 19 nt of homology with the acceptor.[42]

The RNase H and polymerization active sites of the HIV-1 RT are separated by a distance of 16–18 nt of the cDNA–D_{RNA} helix in the RT active site. We envision that the shortest propagation distances for invasion transfer would involve acceptor interaction with an invasion site just as it is leaving the RNase H active site of the RT. Rapid intact-strand branch migration through the substrate cleft of the RT could accomplish transfer over a distance of 17–24 nt. We propose this as the minimum distance of hybrid propagation. The influence of a specific invasion site was lost by 32–64 nt even in the presence of both NC and RNase H, which promote the hybrid propagation reaction. Therefore, this distance range represents the maximum reach of influence of a specific invasion site. Clearly, the many possible sequences and structures of the cDNA–donor and cDNA–acceptor components of the reaction could affect these distances. This expectation is in general agreement with distributions of terminus transfer sites that we and others have determined with substrates having or lacking hairpin structures.[28,40,64–66] Nevertheless, our current results point to a relatively narrow range of influence of a specific invasion site for strand transfer. Moreover, our results are fully consistent with the similarity of recombination frequencies in different sections of the viral genome observed during HIV-1 infection.

Materials and Methods

Materials

DNA oligonucleotides were obtained from Integrated DNA Technologies (Coralville, IA). *Taq* DNA polymerase, deoxy-NTP set, BamHI, SacI, and *E. coli* RNase H were purchased from Invitrogen (San Diego, CA). QIAprep Spin Miniprep Kit was purchased from Qiagen (Valencia, CA).

Polynucleotide kinase, T7 RNA polymerase, ribonucleoside triphosphates, and protector RNase inhibitor were purchased from Roche Applied Science (Indianapolis, IN). The pBluescript I KS (+/−) phagemid vector was purchased from Stratagene (La Jolla, CA). [γ-^{32}P]ATP (6000 Ci/mmol) was purchased from PerkinElmer Life Sciences (Boston, MA). Micro Bio-Spin columns were purchased from Bio-Rad (Hercules, CA). HIV-1 NC (NCp9) was generously provided by Robert J. Gorelick. The HIV-1 RT recombinant heterodimer (p66/P51; specific activity = 38,000 U/mg) was purified as previously described.[66,72] HIV-1 E478Q RT (specific activity = 40,000 U/mg) was generously provided by Stuart F. J. Le Grice. Storm PhosphorImager and Image Quant software version 1.2 were from GE Healthcare (Piscataway, NJ).

Generation of RNA and DNA templates

Donor DNA (D_{DNA}) was purchased from Integrated DNA Technologies and subsequently PAGE purified. D_{RNA} was created with the use of the pD0 plasmid as a template for PCR amplification along with the primers PCIS 5 (5′-TGGTAAACATTCTTGAGTGCTCGATCTGATGTAAGCTTAGAC-3′) and PCIS 6 (5′-GTAATACGACGACTCACTATAGGGCGAATTGGAGCTCCTCAC-3′), which introduced base substitutions and the T7 RNA polymerase promoter.[40,55] (See Table 1.) PCR products were gel purified in Ultrapure™ Low Melting Point Agarose and isolated with a QIAquick Gel Extraction Kit. Gel-purified PCR products were used as templates for T7 RNA polymerase-catalyzed *in vitro* run-off transcription. Full-length D_{RNA} products were PAGE purified. Throughout the text, specific nucleotides within the templates are referred to by number (Fig. 1; Table 1). The numbering system is based on the final nucleotide at the 3′ end of the donor template, numbered 1, which indicates the first nucleotide after the PCIS. Numbers then increase toward the 5′ end of the donor template. Homologous and complementary nucleotides in acceptors and primers, respectively, are numbered in a way that corresponds with the donor template.

The acceptor RNA, A_m, which was used in the strand-transfer reactions, was designed to prevent synthesis on the acceptor if the primer exchanged strands from the donor to the acceptor prior to the initiation of synthesis on the donor. A_m has a 3-nt base substitution at positions 18–20, which creates a mismatch with the 3′-terminus of the unextended primers $-PCIS_{20}$ and $+PCIS_{20}$, to prevent initiation of synthesis on the acceptor. A_m also has a U33A base substitution that was required for synthesis, allowing detection of strand-exchange products (see Strand-exchange assays). Generation of A_m required the use of the pA0 plasmid as a template for overlap PCR, with the primers MH47 (5′-GGTTTTCCCAGTCACGACG-3′), PCIS 9 (5′-GGTAAACATTCTTGAGAAGTCGATCTGATGTTAGC-3′), MH48 (5′-GGAACAAAAGCTGGGTACCG-3′), and PCIS 10 (5′-GCTAACATCAGATCGACTTCTCAAGAATGTTTACC-3′).[40,55] Full-length PCR products were digested with restriction enzymes BamHI and SacI and subsequently cloned into the pBluescript I KS (+/−) phagemid vector. The pA plasmid was digested with BamHI and used as a template for run-off transcription with T7 RNA polymerase.

A_m was also used in the strand-exchange assays to account for the influence of the 3-nt acceptor–primer mismatch at positions 18–20 on the kinetics of exchange. The U33A base substitution was employed in the assay to test the 32-nt distance of strand exchange as described in Strand-exchange assays. Other acceptor templates used in the strand-exchange reactions were A_{64}, A_{32}, A_{24}, and A_{17}, which contain a base substitution at nucleotide positions 65, 33, 25, and 18, respectively. The acceptors were otherwise fully complementary with their respective primers (Table 2). Acceptor RNA A_{64} was created using primers PCIS 47 (5′-ACTAATACGACTCACTATAGGGCGAATTGGAGCTCCGATCCTACGAGTATACGTCTCACTACACATCGCAGTACAAGTC-3′) and PCIS 28 (5′-CCGGTTCTATAACGGTATGATGGTAAACATTCTTGAGTGCTCGATCTGATGTAAGCTTAGACTTGTACTGCGATGTGTAGTGAG-3′) in a PCR to generate a template for run-off transcription with T7 RNA polymerase. Acceptor RNA A_{17} was created using primers PCIS 47 (5′-ACTAATACGACTCACTATAGGGCGAATTGGAGCTCCGATCCTACGAGTATACGTCTCACTACACATCGCAGTACAAGTC-3′) and PCIS 54 (5′-CCG GTT CTA TAA CGG TAT GAT GGT AAA CAT TCT TGA GAG CTC GAT CTG ATG TAA GCT TAG ACT TGT ACT GCG ATG TGT AGT GAG-3′) in a PCR to generate a template for run-off transcription with T7 RNA polymerase. Acceptor RNA A_{24} was created using primers PCIS 47 (5′-ACTAATACGACTCACTATAGGGCGAATTGGAGCTCCGATCCTACGAGTATACGTCTCACTACACATCGCAGTACAAGTC-3′) and PCIS 55 (5′-CCG GTT CTA TAA CGG TAT GAT GGT AAA CAT TCT TGA GTG CTC GAA CTG ATG TAA GCT TAG ACT TGT ACT GCG ATG TGT AGT GAG-3′) in a PCR to generate a template for run-off transcription with T7 RNA polymerase. Acceptor RNA A_{32} was created using primers PCIS 47 (5′-ACTAATACGACTCACTATAGGGCGAATTGGAGCTCCGATCCTACGAGTATACGTCTCACTACACATCGCAGTACAAGTC-3′) and PCIS 56 (5′-CCG GTT CTA TAA CGG TAT GAT GGT AAA CAT TCT TGA GTG CTC GAT CTG ATG TTA GCT TAG ACT TGT ACT GCG ATG TGT AGT GAG-3′) in a PCR to generate a template for run-off transcription with T7 RNA polymerase. All full-length acceptor RNA products were PAGE purified.

Preparation of substrates

[γ-^{32}P]ATP (6000 Ci/mmol) was used to radiolabel the following DNA primers: $-PCIS_{17}$ (5′-TGGTAAACATTCTTGAG-3′), $+PCIS_{17}$ (5′-CCGGTTCTATAACGGTATGATGGTAAACATTCTTGAG-3′), $-PCIS_{18}$ (5′-TGGTAAACATTCTTGAGA-3′), $+PCIS_{18}$ (5′-CCGGTTCTATAACGGTATGATGGTAAACATTCTTGAGA-3′), $-PCIS_{20}$ (5′-TGGTAAACATTCTTGAGTGC-3′), $+PCIS_{20}$ (5′-CCGGTTCTATAACGGTATGATGGTAAACATTCTTGAGTGC-3′), $-PCIS_{24}$ (5′-TGGTAAACATTCTTGAGTGCTCGA-3′), $+PCIS_{24}$ (5′-CCGGTTCTATAACGGTATGATGGTAAACATTCTTGAGTGCTCGA-3′), $-PCIS_{32}$ (5′-TGGTAAACATTCTTGAGTGCTCGATCTGATGT-3′), $+PCIS_{32}$ (5′-CCGGTTCTATAACGGTATGATGGTAAACATTCTTGAGTGCTCGATCTGATGT-3′), $-PCIS_{64}$ (5′-TGGTAAACATTCTTGAGTGCTCGATCTGATGTAAGCTTAGACTTGTACTGCGATGTGTAGTGAG-3′), and $+PCIS_{64}$ (5′-CCGGTTCTATAACGGTATGATGGTAAACATTCTTGAGTGCTCGATCTGATGTAAGCTTAGACTTGTACTGCGATGTGTAGTGAG-3′). The primers were separated from unincorporated radionucleotides with Micro Bio-Spin columns (see Table 1).

Strand-transfer assays

Radiolabeled primer (0.64 nM), $-PCIS_{20}$ or $+PCIS_{20}$, was mixed with donor template (4 nM), either D_{RNA} or D_{DNA} as specified in Fig. 2, in 50 mM Tris, pH 8.0, 50 mM KCl,

1 mM DTT, and 1 mM ethylenediaminetetraacetic acid (EDTA), pH 8.0. The solution was heated at 95 °C for 5 min and then slowly cooled to 37 °C. As specified in Fig. 2, NC was added to coat the nucleic acid 100% (one NC binds 7 nt), followed 3 min later by the addition of RT, either WT or E478Q as specified in Fig. 2, to a concentration of 0.16 U/μl. The solution was incubated at 37 °C for 2 min, at which time acceptor RNA A_m (8 nM), $MgCl_2$ (6 mM), and deoxy-NTP (50 μM) were added simultaneously to start the reaction. Strand-transfer reactions were incubated at 37 °C for 1, 5, 15, 30, and 60 min and were stopped with a termination buffer consisting of 90% formamide, 10 mM EDTA, pH 8.0, 0.1% xylene cyanole, and 0.1% bromophenol blue.

Strand-transfer assays with *E. coli* RNase H

Experiments with exogenous *E. coli* RNase H were conducted similarly to the other strand-transfer assays except that *E. coli* RNase H was added to the reaction to a final concentration of either 0.02 or 0.08 U/μl 3 min after the start of the reaction. Reactions were incubated for 30 min and terminated with the same buffer used in the other strand-transfer assays.

Strand-exchange assays

Radiolabeled primer (0.64 nM) was mixed with donor template D_{RNA} (4 nM) in 50 mM Tris, pH 8.0, 50 mM KCl, 1 mM DTT, and 1 mM EDTA, pH 8.0. The solution was heated at 95 °C for 5 min and then slowly cooled to 37 °C. As specified in Figs. 3–6, NC was added to coat the nucleic acid 100% (one NC binds 7 nt), which was followed by the addition of either WT or E478Q RT (as noted in Figs. 3–6) to a concentration of 0.16 U/μl. The solution was incubated at 37 °C for 2 min, at which time acceptor RNA (8 nM), $MgCl_2$ (6 mM), and deoxy-NTP (50 μM) were added simultaneously to start the reaction. Reactions were incubated at 37 °C for 1, 3, 5, 15, and 30 min and were stopped with a termination buffer as described for the strand-transfer assays.

For strand-exchange experiments with the 3-nt mismatch at positions 18–20, only acceptor A_m was used in all reactions with primers designed to allow increasing lengths of hybrid propagation. The lengths tested were 17, 24, 32, and 64 nt, named $-PCIS_{18}$ and $+PCIS_{18}$, $-PCIS_{24}$ and $+PCIS_{24}$, $-PCIS_{32}$ and $+PCIS_{32}$, and $-PCIS_{64}$ and $+PCIS_{64}$, respectively (Table 1). Primers either had or were lacking the PCIS as indicated by the (+) and (−) signs. Primers $-PCIS_{18}$ and $+PCIS_{18}$ had a 1-nt mismatch with the donor, D_{RNA}, which allowed for only 17 bp to form between the primer and the donor template.

In the strand-exchange reactions with complementary primers and acceptors, the following combinations of primers and acceptors were used: $-PCIS_{17}$ or $+PCIS_{17}$ with A_{17}; $-PCIS_{24}$ or $+PCIS_{24}$ with A_{24}; $-PCIS_{32}$ or $+PCIS_{32}$ with A_{32}; and $-PCIS_{64}$ or $+PCIS_{64}$ with A_{64}. These primers were fully complementary with D_{RNA} and their respective acceptor RNAs (Table 1). Only deoxy-ATP (50 μM) was used to limit primer extension in reactions with the primers $-PCIS_{17}$, $+PCIS_{17}$, $-PCIS_{18}$, $+PCIS_{18}$, $-PCIS_{24}$, $+PCIS_{24}$, $-PCIS_{24}$, and $+PCIS_{24}$, and reactions with the primers $-PCIS_{32}$ and $+PCIS_{32}$ were incubated with only deoxy-TTP (50 μM).

Controls for deoxy-NTP incorporation on the acceptor template were conducted in the same manner as the strand-exchange reactions except that the primer was annealed with acceptor RNA (4 nM) instead of D_{RNA} (4 nM). Also, the reactions were started with the simultaneous addition of $MgCl_2$ (6 mM) and deoxy-NTP (50 μM) but no additional acceptor. Controls for non-template-directed deoxy-NTP incorporation were conducted in the same manner as the strand-exchange reactions except that no acceptor was present in the reaction.

Detection and analysis

All reaction products were separated by denaturing PAGE, imaged with a Storm PhosphorImager, and quantitated with Image Quant software version 1.2. Transfer efficiency (TE) was determined with the equation TE = (TP/(DE + TP)), in which TP is the measured intensity of the strand-transfer products and DE is the measured intensity of full-length donor-template extension products. Relative transfer efficiency (RTE) was determined with the equation RTE = (TE of Reactions with PCIS − TE of Reactions without PCIS).

Acknowledgements

This work was supported by the National Institutes of Health (Training Grant in HIV Replication and Pathogenesis 5T32 AI 049815 and GM 049573). We extend special thanks to Dr. Jeffrey DeStefano for critical reading of the manuscript and providing many beneficial comments. We thank the members of the Bambara laboratory, Dr. Baek Kim, Dr. David H. Mathews, and Dr. Lisa M. Demeter, for helpful discussions. We also thank Dr. Robert J. Gorelick for providing NCp9 and Dr. Stuart F. J. Le Grice for providing E478Q RT.

References

1. Boyer, J. C., Bebenek, K. & Kunkel, T. A. (1992). Unequal human immunodeficiency virus type 1 reverse transcriptase error rates with RNA and DNA templates. *Proc. Natl Acad. Sci. USA*, **89**, 6919–6923.
2. DeStefano, J. J., Wu, W., Seehra, J., McCoy, J., Laston, D., Albone, E. *et al.* (1994). Characterization of an RNase H deficient mutant of human immunodeficiency virus-1 reverse transcriptase having an aspartate to asparagine change at position 498. *Biochim. Biophys. Acta*, **1219**, 380–388.
3. Goodenow, M., Huet, T., Saurin, W., Kwok, S., Sninsky, J. & Wain-Hobson, S. (1989). HIV-1 isolates are rapidly evolving quasispecies: evidence for viral mixtures and preferred nucleotide substitutions. *J. Acquired Immune Defic. Syndr.* **2**, 344–352.
4. Huber, H. E., McCoy, J. M., Seehra, J. S. & Richardson, C. C. (1989). Human immunodeficiency virus 1 reverse transcriptase. Template binding, processivity, strand displacement synthesis, and template switching. *J. Biol. Chem.* **264**, 4669–4678.
5. Ji, J. P. & Loeb, L. A. (1992). Fidelity of HIV-1 reverse transcriptase copying RNA *in vitro*. *Biochemistry*, **31**, 954–958.
6. Preston, B. D., Poiesz, B. J. & Loeb, L. A. (1988). Fidelity of HIV-1 reverse transcriptase. *Science*, **242**, 1168–1171.

7. Roberts, J. D., Bebenek, K. & Kunkel, T. A. (1988). The accuracy of reverse transcriptase from HIV-1. *Science*, **242**, 1171–1173.
8. Weber, J. & Grosse, F. (1989). Fidelity of human immunodeficiency virus type I reverse transcriptase in copying natural DNA. *Nucleic Acids Res.* **17**, 1379–1393.
9. Burke, D. S. (1997). Recombination in HIV: an important viral evolutionary strategy. *Emerging Infect. Dis.* **3**, 253–259.
10. Howell, R. M., Fitzgibbon, J. E., Noe, M., Ren, Z. J., Gocke, D. J., Schwartzer, T. A. & Dubin, D. T. (1991). *In vivo* sequence variation of the human immunodeficiency virus type 1 *env* gene: evidence for recombination among variants found in a single individual. *AIDS Res. Hum. Retroviruses*, **7**, 869–876.
11. Hu, W. S. & Temin, H. M. (1990). Genetic consequences of packaging two RNA genomes in one retroviral particle: pseudodiploidy and high rate of genetic recombination. *Proc. Natl Acad. Sci. USA*, **87**, 1556–1560.
12. Quinones-Mateu, M. E., Gao, Y., Ball, S. C., Marozsan, A. J., Abraha, A. & Arts, E. J. (2002). *In vitro* intersubtype recombinants of human immunodeficiency virus type 1: comparison to recent and circulating *in vivo* recombinant forms. *J. Virol.* **76**, 9600–9613.
13. Robertson, D. L., Hahn, B. H. & Sharp, P. M. (1995). Recombination in AIDS viruses. *J. Mol. Evol.* **40**, 249–259.
14. Temin, H. M. (1993). Retrovirus variation and reverse transcription: abnormal strand transfers result in retrovirus genetic variation. *Proc. Natl Acad. Sci. USA*, **90**, 6900–6903.
15. Vartanian, J. P., Meyerhans, A., Asjo, B. & Wain-Hobson, S. (1991). Selection, recombination, and G→A hypermutation of human immunodeficiency virus type 1 genomes. *J. Virol.* **65**, 1779–1788.
16. Hansen, J., Schulze, T. & Moelling, K. (1987). RNase H activity associated with bacterially expressed reverse transcriptase of human T-cell lymphotropic virus III/lymphadenopathy-associated virus. *J. Biol. Chem.* **262**, 12393–12396.
17. Hurwitz, J. & Leis, J. P. (1972). RNA-dependent DNA polymerase activity of RNA tumor viruses: I. Directing influence of DNA in the reaction. *J. Virol.* **9**, 116–129.
18. Leis, J. P. & Hurwitz, J. (1972). RNA-dependent DNA polymerase activity of RNA tumor viruses: II. Directing influence of RNA in the reaction. *J. Virol.* **9**, 130–142.
19. Starnes, M. C. & Cheng, Y. C. (1989). Human immunodeficiency virus reverse transcriptase-associated RNase H activity. *J. Biol. Chem.* **264**, 7073–7077.
20. Telesnitsky, A. & Goff, S. P. (1993). Strong-stop strand transfer during reverse transcription. In (Skalka, A. M. & Goff, S. P., eds), pp. 49–83, Cold Spring Harbor Laboratory, Cold Spring Harbor, NY.
21. Hwang, C. K., Svarovskaia, E. S. & Pathak, V. K. (2001). Dynamic copy choice: steady state between murine leukemia virus polymerase and polymerase-dependent RNase H activity determines frequency of *in vivo* template switching. *Proc. Natl Acad. Sci. USA*, **98**, 12209–12214.
22. Nikolenko, G. N., Svarovskaia, E. S., Delviks, K. A. & Pathak, V. K. (2004). Antiretroviral drug resistance mutations in human immunodeficiency virus type 1 reverse transcriptase increase template-switching frequency. *J. Virol.* **78**, 8761–8770.
23. Svarovskaia, E. S., Delviks, K. A., Hwang, C. K. & Pathak, V. K. (2000). Structural determinants of murine leukemia virus reverse transcriptase that affect the frequency of template switching. *J. Virol.* **74**, 7171–7178.
24. DeStefano, J. J., Bambara, R. A. & Fay, P. J. (1994). The mechanism of human immunodeficiency virus reverse transcriptase-catalyzed strand transfer from internal regions of heteropolymeric RNA templates. *J. Biol. Chem.* **269**, 161–168.
25. DeStefano, J. J., Mallaber, L. M., Rodriguez-Rodriguez, L., Fay, P. J. & Bambara, R. A. (1992). Requirements for strand transfer between internal regions of heteropolymer templates by human immunodeficiency virus reverse transcriptase. *J. Virol.* **66**, 6370–6378.
26. DeStefano, J. J., Roberts, B. & Shriner, D. (1997). The mechanism of retroviral recombination: the role of sequences proximal to the point of strand transfer. *Arch. Virol.* **142**, 1797–1812.
27. Negroni, M. & Buc, H. (2000). Copy-choice recombination by reverse transcriptases: reshuffling of genetic markers mediated by RNA chaperones. *Proc. Natl Acad. Sci. USA*, **97**, 6385–6390.
28. Roda, R. H., Balakrishnan, M., Kim, J. K., Roques, B. P., Fay, P. J. & Bambara, R. A. (2002). Strand transfer occurs in retroviruses by a pause-initiated two-step mechanism. *J. Biol. Chem.* **277**, 46900–46911.
29. DeStefano, J. J., Buiser, R. G., Mallaber, L. M., Bambara, R. A. & Fay, P. J. (1991). Human immunodeficiency virus reverse transcriptase displays a partially processive 3′ to 5′ endonuclease activity. *J. Biol. Chem.* **266**, 24295–24301.
30. Furfine, E. S. & Reardon, J. E. (1991). Reverse transcriptase.RNase H from the human immunodeficiency virus. Relationship of the DNA polymerase and RNA hydrolysis activities. *J. Biol. Chem.* **266**, 406–412.
31. Gopalakrishnan, V., Peliska, J. A. & Benkovic, S. J. (1992). Human immunodeficiency virus type 1 reverse transcriptase: spatial and temporal relationship between the polymerase and RNase H activities. *Proc. Natl Acad. Sci. USA*, **89**, 10763–10767.
32. Mizrahi, V. (1989). Analysis of the ribonuclease H activity of HIV-1 reverse transcriptase using RNA. DNA hybrid substrates derived from the gag region of HIV-1. *Biochemistry*, **28**, 9088–9094.
33. Fuentes, G. M., Palaniappan, C., Fay, P. J. & Bambara, R. A. (1996). Strand displacement synthesis in the central polypurine tract region of HIV-1 promotes DNA to DNA strand transfer recombination. *J. Biol. Chem.* **271**, 29605–29611.
34. Kelleher, C. D. & Champoux, J. J. (2000). RNA degradation and primer selection by Moloney murine leukemia virus reverse transcriptase contribute to the accuracy of plus strand initiation. *J. Biol. Chem.* **275**, 13061–13070.
35. Schultz, S. J., Zhang, M. & Champoux, J. J. (2004). Recognition of internal cleavage sites by retroviral RNases H. *J. Mol. Biol.* **344**, 635–652.
36. Schultz, S. J., Zhang, M. & Champoux, J. J. (2006). Sequence, distance, and accessibility are determinants of 5′-end-directed cleavages by retroviral RNases H. *J. Biol. Chem.* **281**, 1943–1955.
37. Smith, C. M., Smith, J. S. & Roth, M. J. (1999). RNase H requirements for the second strand transfer reaction of human immunodeficiency virus type 1 reverse transcription. *J. Virol.* **73**, 6573–6581.
38. Wisniewski, M., Balakrishnan, M., Palaniappan, C., Fay, P. J. & Bambara, R. A. (2000). Unique progressive cleavage mechanism of HIV reverse transcriptase RNase H. *Proc. Natl Acad. Sci. USA*, **97**, 11978–11983.

39. Wisniewski, M., Balakrishnan, M., Palaniappan, C., Fay, P. J. & Bambara, R. A. (2000). The sequential mechanism of HIV reverse transcriptase RNase H. *J. Biol. Chem.* **275**, 37664–37671.
40. Hanson, M. N., Balakrishnan, M., Roques, B. P. & Bambara, R. A. (2006). Evidence that creation of invasion sites determines the rate of strand transfer mediated by HIV-1 reverse transcriptase. *J. Mol. Biol.* **363**, 878–890.
41. Heath, M. J. & DeStefano, J. J. (2005). A complementary single-stranded docking site is required for enhancement of strand exchange by human immunodeficiency virus nucleocapsid protein on substrates that model viral recombination. *Biochemistry*, **44**, 3915–3925.
42. Song, M., Basu, V. P., Hanson, M. N., Roques, B. P. & Bambara, R. A. (2008). Proximity and branch migration mechanisms in HIV-1 minus strand strong stop DNA transfer. *J. Biol. Chem.* **283**, 3141–3150.
43. Levin, J. G., Guo, J., Rouzina, I. & Musier-Forsyth, K. (2005). Nucleic acid chaperone activity of HIV-1 nucleocapsid protein: critical role in reverse transcription and molecular mechanism. *Prog. Nucleic Acid Res. Mol. Biol.* **80**, 217–286.
44. Peliska, J. A., Balasubramanian, S., Giedroc, D. P. & Benkovic, S. J. (1994). Recombinant HIV-1 nucleocapsid protein accelerates HIV-1 reverse transcriptase catalyzed DNA strand transfer reactions and modulates RNase H activity. *Biochemistry*, **33**, 13817–13823.
45. Stoylov, S. P., Vuilleumier, C., Stoylova, E., De Rocquigny, H., Roques, B. P., Gerard, D. & Mely, Y. (1997). Ordered aggregation of ribonucleic acids by the human immunodeficiency virus type 1 nucleocapsid protein. *Biopolymers*, **41**, 301–312.
46. Dib-Hajj, F., Khan, R. & Giedroc, D. P. (1993). Retroviral nucleocapsid proteins possess potent nucleic acid strand renaturation activity. *Protein Sci.* **2**, 231–243.
47. Guo, J., Wu, T., Anderson, J., Kane, B. F., Johnson, D. G., Gorelick, R. J. *et al.* (2000). Zinc finger structures in the human immunodeficiency virus type 1 nucleocapsid protein facilitate efficient minus- and plus-strand transfer. *J. Virol.* **74**, 8980–8988.
48. You, J. C. & McHenry, C. S. (1993). HIV nucleocapsid protein. Expression in *Escherichia coli*, purification, and characterization. *J. Biol. Chem.* **268**, 16519–16527.
49. Beltz, H., Piemont, E., Schaub, E., Ficheux, D., Roques, B., Darlix, J. L. & Mely, Y. (2004). Role of the structure of the top half of HIV-1 cTAR DNA on the nucleic acid destabilizing activity of the nucleocapsid protein NCp7. *J. Mol. Biol.* **338**, 711–723.
50. Hong, M. K., Harbron, E. J., O'Connor, D. B., Guo, J., Barbara, P. F., Levin, J. G. & Musier-Forsyth, K. (2003). Nucleic acid conformational changes essential for HIV-1 nucleocapsid protein-mediated inhibition of self-priming in minus-strand transfer. *J. Mol. Biol.* **325**, 1–10.
51. Tsuchihashi, Z. & Brown, P. O. (1994). DNA strand exchange and selective DNA annealing promoted by the human immunodeficiency virus type 1 nucleocapsid protein. *J. Virol.* **68**, 5863–5870.
52. Urbaneja, M. A., Wu, M., Casas-Finet, J. R. & Karpel, R. L. (2002). HIV-1 nucleocapsid protein as a nucleic acid chaperone: spectroscopic study of its helix-destabilizing properties, structural binding specificity, and annealing activity. *J. Mol. Biol.* **318**, 749–764.
53. Williams, M. C., Rouzina, I., Wenner, J. R., Gorelick, R. J., Musier-Forsyth, K. & Bloomfield, V. A. (2001). Mechanism for nucleic acid chaperone activity of HIV-1 nucleocapsid protein revealed by single molecule stretching. *Proc. Natl Acad. Sci. USA*, **98**, 6121–6126.
54. Chen, Y., Balakrishnan, M., Roques, B. P. & Bambara, R. A. (2005). Acceptor RNA cleavage profile supports an invasion mechanism for HIV-1 minus strand transfer. *J. Biol. Chem.* **280**, 14443–14452.
55. Hanson, M. N., Balakrishnan, M., Roques, B. P. & Bambara, R. A. (2005). Effects of donor and acceptor RNA structures on the mechanism of strand transfer by HIV-1 reverse transcriptase. *J. Mol. Biol.* **353**, 772–787.
56. Lapadat-Tapolsky, M., De Rocquigny, H., Van Gent, D., Roques, B., Plasterk, R. & Darlix, J. L. (1993). Interactions between HIV-1 nucleocapsid protein and viral DNA may have important functions in the viral life cycle. *Nucleic Acids Res.* **21**, 831–839.
57. Lapadat-Tapolsky, M., Pernelle, C., Borie, C. & Darlix, J. L. (1995). Analysis of the nucleic acid annealing activities of nucleocapsid protein from HIV-1. *Nucleic Acids Res.* **23**, 2434–2441.
58. You, J. C. & McHenry, C. S. (1994). Human immunodeficiency virus nucleocapsid protein accelerates strand transfer of the terminally redundant sequences involved in reverse transcription. *J. Biol. Chem.* **269**, 31491–31495.
59. Chen, J., Rhodes, T. D. & Hu, W. S. (2005). Comparison of the genetic recombination rates of human immunodeficiency virus type 1 in macrophages and T cells. *J. Virol.* **79**, 9337–9340.
60. Jetzt, A. E., Yu, H., Klarmann, G. J., Ron, Y., Preston, B. D. & Dougherty, J. P. (2000). High rate of recombination throughout the human immunodeficiency virus type 1 genome. *J. Virol.* **74**, 1234–1240.
61. Levy, D. N., Aldrovandi, G. M., Kutsch, O. & Shaw, G. M. (2004). Dynamics of HIV-1 recombination in its natural target cells. *Proc. Natl Acad. Sci. USA*, **101**, 4204–4209.
62. Onafuwa, A., An, W., Robson, N. D. & Telesnitsky, A. (2003). Human immunodeficiency virus type 1 genetic recombination is more frequent than that of Moloney murine leukemia virus despite similar template switching rates. *J. Virol.* **77**, 4577–4587.
63. Zhuang, J., Jetzt, A. E., Sun, G., Yu, H., Klarmann, G., Ron, Y. *et al.* (2002). Human immunodeficiency virus type 1 recombination: rate, fidelity, and putative hot spots. *J. Virol.* **76**, 11273–11282.
64. Balakrishnan, M., Roques, B. P., Fay, P. J. & Bambara, R. A. (2003). Template dimerization promotes an acceptor invasion-induced transfer mechanism during human immunodeficiency virus type 1 minus-strand synthesis. *J. Virol.* **77**, 4710–4721.
65. Gao, L., Balakrishnan, M., Roques, B. P. & Bambara, R. A. (2007). Insights into the multiple roles of pausing in HIV-1 reverse transcriptase-promoted strand transfers. *J. Biol. Chem.* **282**, 6222–6231.
66. Roda, R. H., Balakrishnan, M., Hanson, M. N., Wohrl, B. M., Le Grice, S. F., Roques, B. P. *et al.* (2003). Role of the reverse transcriptase, nucleocapsid protein, and template structure in the two-step transfer mechanism in retroviral recombination. *J. Biol. Chem.* **278**, 31536–31546.
67. Chen, Y., Balakrishnan, M., Roques, B. P. & Bambara, R. A. (2003). Steps of the acceptor invasion mechanism for HIV-1 minus strand strong stop transfer. *J. Biol. Chem.* **278**, 38368–38375.
68. Derebail, S. S. & DeStefano, J. J. (2004). Mechanistic analysis of pause site-dependent and -independent recombinogenic strand transfer from structurally

diverse regions of the HIV genome. *J. Biol. Chem.* **279**, 47446–47454.
69. Moumen, A., Polomack, L., Unge, T., Veron, M., Buc, H. & Negroni, M. (2003). Evidence for a mechanism of recombination during reverse transcription dependent on the structure of the acceptor RNA. *J. Biol. Chem.* **278**, 15973–15982.
70. Basu, V. P., Song, M., Gao, L., Rigby, S. T., Hanson, M. N. & Bambara, R. A. (2008). Strand transfer events during HIV-1 reverse transcription. *Virus Res.* **134**, 19–38.
71. Purohit, V., Balakrishnan, M., Kim, B. & Bambara, R. A. (2005). Evidence that HIV-1 reverse transcriptase employs the DNA 3′ end-directed primary/secondary RNase H cleavage mechanism during synthesis and strand transfer. *J. Biol. Chem.* **280**, 40534–40543.
72. Pandey, V. N., Kaushik, N., Rege, N., Sarafianos, S. G., Yadav, P. N. & Modak, M. J. (1996). Role of methionine 184 of human immunodeficiency virus type-1 reverse transcriptase in the polymerase function and fidelity of DNA synthesis. *Biochemistry*, **35**, 2168–2179.